Nearly Linear Rh(I) Aggregates. Chemical and Spectroscopic Behavior of $[Rh_3(CNCH_3)_6\{\mu\text{-}(Ph_2PCH_2)_2PPh\}_2]^{3+}$ and Its Oxidation Products

Alan L. Balch,* L. Alan Fossett, Jeffrey K. Nagle, and Marilyn M. Olmstead

Contribution from the Department of Chemistry, University of California, Davis, California 95616. *Received September 14, 1987*

Abstract: The reaction of $[Rh_3(\mu\text{-}Cl)Cl(CO)_3(\mu\text{-dpmp})_2]^+$ (**2**) (dpmp is bis(diphenylphosphinomethyl)phenylphosphine) with excess methyl isocyanide yields green $[Rh_3(CNCH_3)_6(\mu\text{-dpmp})_2]^{3+}$: λ_{max} (absorption) 670 nm, λ_{max} (emission) 815 nm (in dichloromethane at 25 °C). Green $[Rh_3(CNC_3)_6\{\mu\text{-}((C_6H_5)_2PCH_2)_2P(C_6H_5)\}_2][PF_6]_3\cdot 1.3CH_2Cl_2$ crystallizes from dichloromethane/ethyl ether in the triclinic space group $P\bar{1}$ with a = 14.111 (4) Å, b = 16.654 (5) Å, c = 21.644 (6) Å, α = 91.42 (2)°, β = 102.43 (2)°, γ = 103.71 (2)° at 130 K. Least-squares refinement of 826 parameters with 8971 reflections yielded R = 0.095 and R_w = 0.107. The structure of the cation consists of three nearly planar $RhP_2(CNCH_3)_2$ units connected through the dpmp bridge with Rh–Rh separations of 3.090 (1) and 3.106 (1) Å. Addition of halogens or carbon tetrahalides to **2** produces two-fragment, three-center oxidative additions to form $[Rh_3(CNCH_3)_6(\mu\text{-dpmp})_2X_2]^{3+}$ (X = I, Br, Cl), which have been isolated as the hexafluorophosphate salts and spectroscopically characterized. Electrochemical oxidation of **2** shows two one-electron oxidations. The oxidation products, $[Rh_3(CNCH_3)_6(\mu\text{-dpmp})_2]^{4+}$ and $[Rh_3(CNCH_3)_6(\mu\text{-dpmp})_2]^{5+}$, have been characterized by electronic and ESR spectroscopy and by chemical reactivity. The nature of the Rh–Rh interactions and the chemical behavior of these trinuclear species are explained by a simple molecular orbital picture involving the out-of-plane filled d_{z^2} and empty p_z orbitals.

The intense blue, violet, and green colors seen in concentrated solutions of $Rh(CNR)_4^+$, which as a planar, monomeric ion is yellow, have been shown to be due to the formation of dimers and trimers that are connected solely through Rh–Rh bonding.[1-4] The formation of these oligomers is a reversible process. However, using suitably designed bridging ligands, it is possible to stabilize the oligomeric forms. With isocyanide bridges such as diisocyanopropane, it is possible to stabilize the dimeric species,[5-8] e.g., $[Rh_2\{CN(CH_2)_3NC\}_4]^{2+}$, and observe their condensation to form chains of even numbers (four, six, and eight) of rhodium(I) ions.[9] With the bridging diphosphine, bis(diphenylphosphino)methane (dpm), similar dimers form, but the bulky phenyl groups prevent further polymerization.[10-12] Thus, $[Rh_2(CNR)_4(\mu\text{-dpm})_2]^+$ (**1**) remains a dimer under all observed conditions.

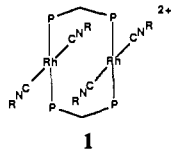

1

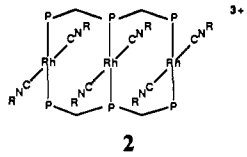

2

Here we report on the preparation and chemical behavior of the first isolated trinuclear complex, **2**, of this type. For this we use the small-bite triphosphine, bis(diphenylphosphinomethyl)-phenylphosphine (dpmp).[13] While some information on trirhodium species of this type has been available, previous work was strongly limited by the ease of dissociation of the trinuclear units. The present work allows for direct comparison of **1** and **2** and shows how a simple bonding model that focuses on the overlap of the out-of-plane orbitals can account for the differences between **1**, **2**, and corresponding monomers.

Results

Synthesis of 2. As with all other dpmp-bridged trirhodium complexes, the entry to the preparation of **2** is $[Rh_3(CO)_3(\mu\text{-}Cl)Cl(\mu\text{-dpmp})_2][BPh_4]$.[13,14] Treatment of a dichloromethane solution of this rose-colored cation with 6 molar equiv of methyl isocyanide yields an air-sensitive, green solution from which green crystals of $[Rh_3(CNCH_3)_6(\mu\text{-dpmp})_2][PF_6]_3$ (**2**) are obtained by the addition of methanolic ammonium hexafluorophosphate. Spectroscopic data for this and other new compounds are given in Table I. The ^{31}P NMR spectrum is characteristic of compounds with identical environments for the two end $Ph_2PRhPPh_2$ groups. The infrared spectrum shows a single isocyanide stretching vibration in the region characteristic of Rh(I) complexes.[2,10] The electronic absorption spectrum of the cation is shown in Figure 1. There is an intense absorption maximum at 674 nm. Like **1**,[15] **2** is also luminescent. The emission is shown as the dashed trace in Figure 1. An excitation spectrum taken for the 815 emission shows a maximum at 674 nm that is coincident with the dominant, low-energy absorption feature. On the basis of the small Stokes shift (2600 ca^{-1} for 815 emission) of the emission, we ascribe it to fluorescence. Detector limitations did not allow us to observe the phosphorescence that is expected at lower energies. A similar complex with *n*-butyl isocyanide ligands has been prepared. It shows similar properties.

The Crystal and Molecular Structure of $[Rh_3(CNCH_3)_6(\mu\text{-dpmp})_2][PF_6]_3\cdot 1.3CH_2Cl_2$. In addition to the well-behaved cation, the solid contains three disordered hexafluorophosphate ions and three partially occupied sites for dichloromethane molecules. A view of the cation, with its numbering scheme, is given in Figure 2. Atomic positional parameters are given in Table II. Tables III and IV contain selected interatomic distances and angles, respectively.

While the cation has no crystallographically imposed symmetry, the $Rh_3(CNCH_3)_6$ unit is nearly planar. A projection of that portion with some dimensions is shown in Figure 3.

The cation consists of three planar d^8 $P_2Rh^I(CNCH_3)_2$ units held together by the two bridging dpmp ligands. The two Rh···Rh

(1) Malatesta, L.; Vallarino, L. *J. Chem. Soc.* **1956**, 1867.
(2) Dart, J. W.; Lloyd, M. K.; Mason, R.; McCleverty, J. A. *J. Chem. soc., Dalton Trans.* **1973**, 2039.
(3) Mann, K. R.; Gordon, J. G., II; Gray, H. B. *J. Am. Chem. Soc.* **1975**, *97*, 3553.
(4) Mann, K. R.; Lewis, N. S.; Williams, R. M.; Gray, H. B.; Gordon, J. G. II *Inorg. Chem.* **1978**, *17*, 828.
(5) Lewis, N. S.; Mann, K. R.; Gordon, J. G., II; Gray, H. B. *J. Am. Chem. Soc.* **1976**, *98*, 7462.
(6) Kawakami, K.; Okajma, M; Tanaka, T. *Bull. Chem. Soc. Jpn.* **1978**, *51*, 2327.
(7) Powell, J.; Yaneff, P. V. *J. Organomet. Chem.* **1979**, *179*, 101.
(8) Mann, K. R.; Thick, J. A.; Bell, R. A.; Coyle, C. L.; Gray, H. B. *Inorg. Chem.* **1980**, *19*, 2462.
(9) Sigal, I. S.; Gray, H. B. *J. Am. Chem. Soc.* **1981**, *103*, 2220.
(10) Balch, A. L. *J. Am. Chem. Soc.* **1976**, *98*, 8049.
(11) Balch, A. L.; Tulyathan, B. *Inorg. Chem.* **1977**, *16*, 2840.
(12) Balch, A. L.; Labadie, J. W.; Delker, G. *Inorg. Chem.* **1979**, *18*, 1224.
(13) Guimerans, R. R.; Olmstead, M. M.; Balch, A. L. *J. Am. Chem. Soc.* **1983**, *105*, 1677.
(14) Balch, A. L.; Fossett, L. A.; Guimerans, R. R.; Olmstead, M. M.; Reedy, P. E., Jr.; Wood, F. E. *Inorg. Chem.* **1986**, *25*, 1248.
(15) Fordyce, W. A.; Crosby, G. A. *J. Am. Chem. Soc.* **1982**, *104*, 985.

0002-7863/88/1510-6732$01.50/0

Table I. Spectroscopic Data

compd	IR[a] ν(CN), nm	^{31}P NMR[b,c] δ, ppm	^{1}J(Rh,P), Hz	absorption[b] λ_{max}, nm (ϵ, M^{-1} cm^{-1})	emission[b] λ_{max}, nm
$[Rh_3(CNCH_3)_6(\mu\text{-dpmp})_2][PF_6]_3$	2170	19.5	118	674 (30000), 455 (2500)	815
		17.4	116	385 (3800), 323 (1700)	
$[Rh_3(CNC_4H_9)_6(\mu\text{-dpmp})_2][PF_6]_3$	2160	18.2	120	674 (24000), 380 (3400)	804
		16.8	120	325 (1400)	
$[Rh_3(CNCH_3)_6(\mu\text{-dpmp})_2Cl_2][PF_6]_3$	2210	3.6	90	586 (36000), 437 (500)	732, 800
		10.7	95	364 (12000), 323 (14000)	
$[Rh_3(CNCH_3)_6(\mu\text{-dpmp})_2Br_2][PF_6]_3$	2207	2.8	90	610 (63000), 456 (7100)	740, 800
		10.0	94	374 (12000), 328 (9800)	
$[Rh_3(CNCH_3)_6(\mu\text{-dpmp})_2I_2][PF_6]_3$	2201	0.8	90	662 (85000), 500 (4500)	none
		9.1	94	435 (7000), 375 (20000)	
				326 (14000)	

[a] Mineral oil mull. [b] Dichloromethane solution. [c] Apparent P–P coupling of ca. 30 Hz is also present.

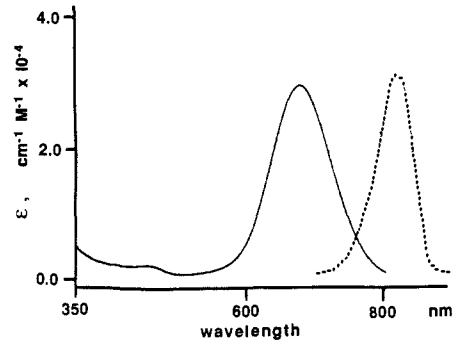

Figure 1. The electronic spectra of $[Rh_3(CNCH_3)_6(\mu\text{-dpmp})_2][PF_6]_3$ (**2**) in dichloromethane at 25 °C: solid line, absorption; dashed line, emission in arbitrary units.

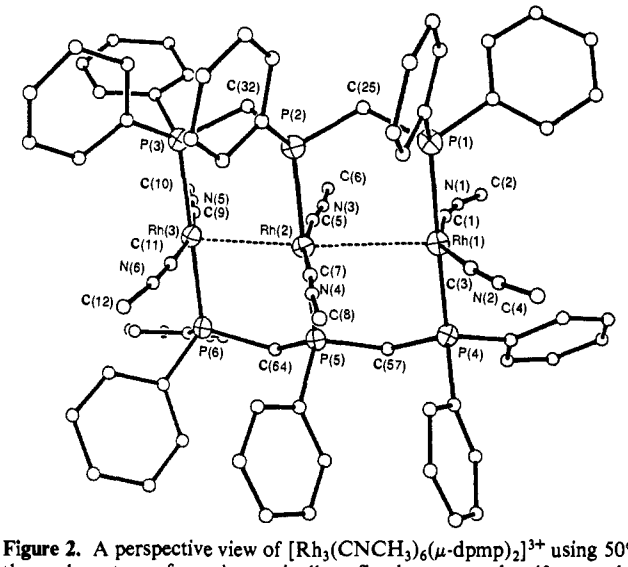

Figure 2. A perspective view of $[Rh_3(CNCH_3)_6(\mu\text{-dpmp})_2]^{3+}$ using 50% thermal contours for anisotropically refined atoms and uniform, arbitrarily sized circles for other atoms.

distances, 3.106 (1) and 3.090 (1) Å, are similar. These distances are somewhat shorter than the range, 3.19–3.26 Å, found for other related, bridged complexes, $[Rh_2(\mu\text{-dpm})_2(\mu\text{-1,8-diisocyanomenthane})_2]^{2+}$ (**3**)[16] and $[Rh_2(1,3\text{-diisocyanopropane})_4]^{2+}$,[8] as well as for the unbridged Rh–Rh bonded dimers[4,17] such as $[Rh_2(CNC_6H_5)_8]^{2+}$. Although these distances are longer than the general range found for Rh–Rh single bonds (2.6–2.8 Å), the Rh···Rh interactions within **2** are certainly attractive and spectroscopically significant. The Rh···Rh···Rh angle is 160.2 (1)°.

The bonding within the isocyanides and bridging phosphine ligands appears quite normal. The Rh–C bonds in **2** are all similar

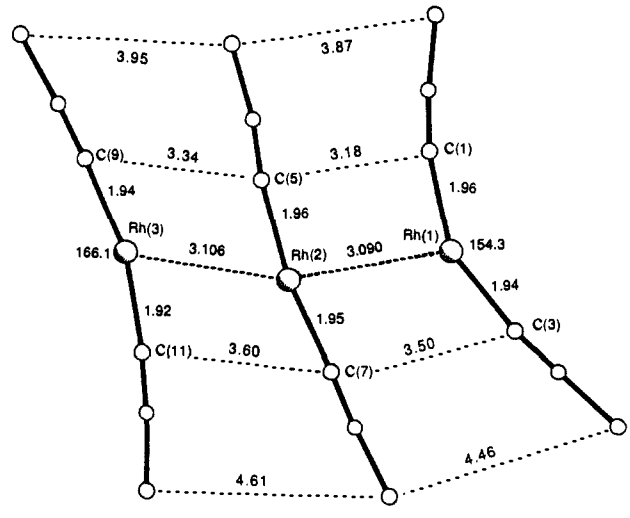

Figure 3. The $Rh_3(CNCH_3)_6$ core of $[Rh_3(CNCH_3)_6(\mu\text{-dpmp})_2]^{3+}$ showing some interatomic contacts.

in length (range 1.93 (1)–1.97 (1) Å) and similar to those (1.953 Å) in **3**.[16] The Rh–P bond lengths (2.298 (3), 2.328 (4) Å) are also comparable to the 2.318-Å distance found in **3**.[16]

There is evidence for crowding within the $Rh_3(CNCH_3)_6$ core. The four isocyanide ligands at the end of the cation bend away from the center of the molecules so that the normal linear C–Rh–C angles are compressed to 154.3 (6)° at Rh(1) and 166.1 (7)° at Rh(3). The central C(5)–Rh(2)–C(7) angle is 170.0 (6)°. These distortions are necessary in order to accommodate the methyl groups of the isocyanate ligands. Notice that the nonbonded C···C separation between the rhodium bonded carbons falls in the range 3.18–3.60 Å, which is lower than the sum of the van der Waals radii for two methyl groups (4.0 Å),[18] but as a result of the induced distortions, the C(methyl)···C(methyl) separations (range, 3.87–4.61 Å) are much closer to or larger than the expected van der Waals separation between methyl groups.

Oxidative Additions. Treatment of **2** with iodine produces oxidative addition to each end of the trirhodium chain as shown in eq 1. The green product is obtained in 94% yield. Its infrared

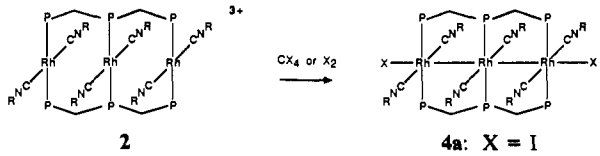

(1)

2

4a: X = I
b: X = Br
c: X = Cl

spectrum shows only a terminal isocyanide stretch at 2201 cm^{-1}. The 31-cm^{-1} increase in ν(CN) for the product relative to **2** is entirely consistent with the axial oxidative addition. The ^{31}P NMR spectrum of the product shows that only two types of phosphorus

(16) Boyd, D. C.; Matsch, P. A.; Mixa, M. M.; Mann, K. R. *Inorg. Chem.* **1986**, *25*, 3333.
(17) Enders, H.; Gottstein, N.; Keller, H. J.; Martin, R.; Rodemer, W.; Steiger, W. *Z. Naturforsch.* **1979**, *34b*, 827.
(18) Pauling, L. In *The Nature of the Chemical Bond*; Cornell University Press: Ithaca, NY, 1960; p 260.

Table II. Atomic Coordinates ($\times 10^4$) and Isotropic Thermal Parameters ($Å^2 \times 10^3$) for $[Rh_3(CNCH_3)_6(\mu\text{-dpmp})_2][PF_6]_3 \cdot 1.3CH_2Cl_2$

	x	y	z	U[a]		x	y	z	U[a]
Rh(1)	2090 (1)	1758 (1)	2335 (1)	24 (1)*	C(57)	834 (9)	2977 (8)	1396 (6)	34 (3)
Rh(2)	467 (1)	2361 (1)	2837 (1)	23 (1)*	C(58)	1092 (9)	4403 (7)	2297 (5)	30 (3)
Rh(3)	−1631 (1)	2496 (1)	2989 (1)	41 (1)*	C(59)	1358 (10)	4949 (8)	1814 (7)	45 (3)
P(1)	1983 (2)	690 (2)	2990 (1)	24 (1)*	C(60)	1804 (10)	5775 (8)	1978 (7)	45 (3)
P(2)	405 (2)	1319 (2)	3518 (1)	22 (1)*	C(61)	1985 (12)	6079 (10)	2606 (7)	56 (4)
P(3)	−1671 (3)	1489 (2)	3708 (2)	35 (1)*	C(62)	1698 (11)	5577 (9)	3070 (7)	52 (4)
P(4)	2042 (2)	2708 (2)	1576 (2)	28 (1)*	C(63)	1278 (10)	4732 (8)	2905 (6)	41 (3)
P(5)	429 (2)	3313 (2)	2082 (1)	26 (1)*	C(64)	−842 (9)	3374 (8)	1697 (5)	31 (3)
P(6)	−1651 (3)	3481 (2)	2245 (2)	40 (1)*	C(65)	−2854 (10)	3415 (8)	1710 (6)	40 (3)
N(1)	520 (8)	476 (6)	1357 (5)	36 (3)	C(66)	−3172 (16)	2921 (13)	1195 (10)	89 (6)
N(2)	4348 (9)	2510 (7)	2925 (5)	51 (3)	C(67)	−4183 (18)	2816 (15)	804 (11)	107 (7)
N(3)	−1257 (7)	1135 (6)	1872 (4)	29 (2)	C(68)	−4773 (16)	3298 (12)	1027 (10)	89 (6)
N(4)	2477 (8)	3413 (6)	3684 (5)	37 (3)	C(69)	−4474 (19)	3720 (16)	1537 (12)	119 (8)
N(5)	−3624 (10)	1424 (8)	2177 (6)	65 (4)	C(70)	−3500 (15)	3820 (12)	1926 (10)	86 (6)
N(6)	−101 (10)	3730 (8)	3995 (6)	62 (4)	C(71)	−1300 (11)	4577 (9)	2542 (7)	51 (4)
C(1)	1010 (9)	987 (7)	1722 (5)	31 (3)	C(72)	−1017 (12)	5192 (10)	2185 (8)	59 (4)
C(2)	−20 (15)	−246 (12)	921 (9)	82 (6)	C(73)	−854 (16)	6043 (13)	2428 (10)	91 (6)
C(3)	3480 (10)	2272 (8)	2434 (6)	38 (3)	C(74)	−1058 (20)	6152 (18)	2976 (12)	129 (9)
C(4)	5432 (16)	2848 (13)	3119 (10)	94 (6)	C(75)	−1396 (23)	5560 (19)	3289 (16)	163 (12)
C(5)	−661 (9)	1601 (7)	2249 (5)	26 (3)	C(76)	−1551 (18)	4734 (15)	3104 (11)	110 (7)
C(6)	−2117 (13)	572 (11)	1420 (8)	65 (5)	C(77)	3119 (23)	4125 (18)	8948 (14)	51 (8)
C(7)	1731 (10)	3016 (8)	3359 (6)	35 (3)	C(78)	5580 (27)	3367 (22)	6150 (17)	71 (10)
C(8)	3410 (12)	3870 (10)	4065 (7)	55 (4)	C(79)	5813	2188	8650	93 (21)
C(9)	−2868 (11)	1810 (9)	2464 (7)	47 (4)	P(7)	1729 (3)	1597 (2)	7632 (2)	43 (1)*
C(10)	−4601 (18)	907 (14)	1830 (11)	103 (7)	P(8A)	6471 (8)	4361 (5)	4641 (4)	46 (3)*
C(11)	−627 (10)	3270 (8)	3605 (6)	40 (3)	P(8B)	7108 (10)	4495 (5)	4589 (4)	44 (4)*
C(12)	536 (15)	4370 (12)	4503 (10)	84 (6)	P(9)	5185 (10)	285 (7)	9938 (7)	83 (6)*
C(13)	2059 (9)	−277 (7)	2599 (5)	28 (3)	P(10)	9617 (14)	4376 (12)	9850 (7)	150 (10)*
C(14)	1401 (11)	−1031 (8)	2605 (6)	44 (3)	F(1A)	2363 (11)	2270 (9)	7254 (6)	61 (6)*
C(15)	1484 (12)	−1720 (10)	2278 (7)	58 (4)	F(2A)	1016 (11)	987 (10)	7945 (7)	75 (7)*
C(16)	2195 (11)	−1677 (9)	1947 (7)	51 (4)	F(3A)	819 (12)	2073 (9)	7367 (8)	75 (7)*
C(17)	2845 (13)	−928 (10)	1942 (7)	62 (4)	F(4A)	2033 (17)	2261 (12)	8202 (8)	113 (10)*
C(18)	2778 (10)	−233 (9)	2260 (6)	42 (3)	F(5A)	2587 (13)	1201 (11)	7843 (10)	98 (9)*
C(19)	2846 (9)	753 (7)	3755 (5)	26 (3)	F(6A)	1279 (11)	1023 (9)	6985 (7)	69 (6)*
C(20)	3328 (10)	1523 (9)	4072 (6)	44 (3)	F(1B)	916 (14)	1562 (14)	7057 (9)	55 (8)*
C(21)	3994 (13)	1587 (11)	4700 (8)	64 (4)	F(2B)	2371 (32)	1295 (30)	7199 (13)	165 (25)*
C(22)	4060 (12)	853 (9)	4971 (8)	58 (4)	F(3B)	2583 (17)	1549 (14)	8290 (9)	69 (9)*
C(23)	3566 (11)	91 (10)	4671 (7)	55 (4)	F(4B)	2216 (19)	2533 (22)	7612 (18)	150 (18)*
C(24)	2966 (10)	60 (9)	4066 (6)	43 (3)	F(5B)	1306 (22)	603 (13)	7658 (15)	122 (14)*
C(25)	749 (8)	428 (7)	3207 (5)	26 (3)	F(6B)	1026 (19)	1823 (26)	8056 (15)	151 (19)*
C(26)	1083 (9)	1513 (7)	4352 (5)	26 (3)	F(7A)	7014 (11)	4332 (10)	5380 (7)	50 (6)*
C(27)	1293 (9)	2290 (8)	4654 (6)	32 (3)	F(8A)	5987 (16)	3377 (11)	4591 (9)	77 (9)*
C(28)	1750 (11)	2440 (9)	5296 (7)	49 (4)	F(9A)	5985 (20)	4408 (10)	3918 (8)	81 (10)*
C(29)	2005 (11)	1804 (9)	5640 (7)	47 (4)	F(10A)	6980 (11)	5325 (8)	4674 (7)	50 (6)*
C(30)	1796 (10)	1022 (8)	5334 (6)	42 (3)	F(11A)	5557 (16)	4504 (14)	4889 (10)	81 (10)*
C(31)	1346 (9)	887 (8)	4700 (6)	33 (3)	F(12A)	7389 (21)	4147 (15)	4400 (11)	75 (12)*
C(32)	−881 (8)	803 (7)	3574 (5)	26 (3)	F(7B)	6902 (15)	4487 (12)	3819 (9)	74 (8)*
C(33)	−1340 (10)	1820 (8)	4548 (6)	41 (3)	F(8B)	8232 (18)	4463 (12)	4572 (9)	65 (9)*
C(34)	−886 (10)	1377 (8)	5012 (6)	37 (3)	F(9B)	5969 (13)	4515 (12)	4613 (10)	65 (9)*
C(35)	−662 (12)	1652 (10)	5657 (7)	56 (4)	F(10B)	7464 (12)	5510 (9)	4665 (8)	58 (7)*
C(36)	−937 (16)	2347 (13)	5839 (11)	96 (6)	F(11B)	7408 (12)	4484 (10)	5336 (6)	47 (6)*
C(37)	−1495 (16)	2746 (13)	5370 (10)	93 (6)	F(12B)	6766 (13)	3504 (8)	4545 (7)	57 (7)*
C(38)	−1569 (13)	2549 (11)	4740 (8)	68 (5)	F(13)	4062 (38)	451 (35)	9413 (15)	282 (33)*
C(39)	−2899 (11)	772 (9)	3596 (7)	46 (3)	F(14)	4482 (19)	87 (19)	10454 (11)	95 (13)*
C(40)	−3681 (12)	1065 (11)	3804 (8)	63 (4)	F(15)	5891 (22)	−183 (24)	10354 (10)	242 (21)*
C(41)	−4667 (14)	447 (11)	3640 (8)	75 (5)	F(16)	4555 (30)	−531 (17)	9604 (12)	179 (19)*
C(42)	−4815 (16)	−232 (12)	3362 (9)	85 (6)	F(17)	5866 (29)	362 (22)	9388 (17)	147 (19)*
C(43)	−4131 (13)	−536 (11)	3204 (8)	65 (5)	F(18)	5718 (25)	1060 (15)	10341 (16)	172 (18)*
C(44)	−3158 (12)	−20 (9)	3315 (7)	53 (4)	F(19)	9755 (15)	4850 (13)	10501 (7)	186 (11)*
C(45)	2939 (9)	3734 (7)	1692 (5)	30 (3)	F(20)	10721 (21)	4291 (18)	10180 (11)	116 (14)*
C(46)	3123 (9)	4176 (8)	1203 (6)	35 (3)	F(21)	8529 (28)	4460 (34)	9555 (12)	208 (27)*
C(47)	3717 (11)	4960 (9)	1293 (7)	53 (4)	F(22)	9701 (29)	3709 (31)	9263 (12)	229 (26)*
C(48)	4207 (12)	5319 (11)	1913 (7)	62 (4)	F(23)	9587 (56)	3329 (45)	9979 (32)	602 (55)*
C(49)	4045 (12)	4877 (10)	2434 (8)	61 (4)	Cl(1)	4171 (7)	3872 (10)	9408 (8)	163 (8)*
C(50)	3388 (11)	4064 (9)	2301 (7)	49 (4)	Cl(2)	2462 (9)	4507 (6)	9380 (4)	87 (5)*
C(51)	2162 (10)	2278 (8)	814 (6)	36 (3)	Cl(3)	6052 (11)	2458 (7)	6139 (5)	125 (6)*
C(52)	1692 (11)	2463 (9)	227 (7)	50 (4)	Cl(4)	4590 (12)	3216 (10)	6368 (12)	217 (12)*
C(53)	1865 (12)	2166 (10)	−322 (8)	61 (4)	Cl(5)	5556 (11)	2407 (7)	7993 (9)	80 (7)*
C(54)	2503 (13)	1652 (10)	−290 (8)	66 (5)	Cl(6A)	6557	2885	9218	43 (5)
C(55)	2969 (14)	1455 (11)	298 (8)	75 (5)	Cl(6B)	4876	1447	8877	121 (14)
C(56)	2791 (11)	1756 (9)	844 (7)	50 (4)					

[a] an asterisk indicates equivalent isotropic U defined as one-third of the trace of the orthongalized U_{ij} tensor.

nuclei are present in the product. Interestingly the chemical shifts for the terminal and internal phosphorus atoms are reversed in **4a** relative to **2**. The decrease in $^1J(Rh_1P)$ for both the terminal and the internal phosphorus resonances indicates that the oxidation affects all three rhodium centers similarly. The electronic spectrum of **4a** (shown in Figure 4) is dominated by an intense

Table III. Selected Interactomic Distances in $[Rh_3(CNCH_3)_6(\mu\text{-dpmp})_2][PF_6]_3$

	At Rh(1)		
Rh(1)···Rh(2)	3.090 (1)	Rh(1)···Rh(3)	6.104 (1)
Rh(1)–P(1)	2.298 (3)	Rh(1)–P(4)	2.311 (3)
Rh(1)–C(1)	1.96 (1)	Rh(1)–C(3)	1.94 (1)
	At Rh(2)		
Rh(2)···Rh(1)	3.090 (1)	Rh(2)···Rh(3)	3.106 (1)
Rh(2)–P(2)	2.303 (3)	Rh(2)–P(5)	2.305 (3)
Rh(2)–C(5)	1.96 (1)	Rh(2)–C(7)	1.95 (1)
	At Rh(3)		
Rh(3)···Rh(2)	3.106 (1)		
Rh(3)–P(3)	2.314 (4)	Rh(3)–P(6)	2.33 (4)
Rh(3)–C(9)	1.94 (1)	Rh(3)–C(11)	1.92 (1)
	In Isocyanide Ligands		
C(1)–N(1)	1.13 (1)	C(7)–N(4)	1.17 (1)
C(3)–N(2)	1.17 (2)	C(9)–N(5)	1.14 (2)
C(5)–N(3)	1.16 (1)	C(11)–N(6)	1.13 (2)
	Between Ligand Atoms		
P(1)···P(2)	3.082 (9)	P(4)···P(5)	3.082 (9)
P(2)···P(3)	3.120 (9)	P(5)···P(6)	3.107 (6)
C(1)···C(5)	3.18 (2)	C(3)···C(7)	3.50 (2)
C(5)···C(9)	3.34 (2)	C(7)···C(11)	3.60 (2)
N(1)···N(3)	3.34 (1)	N(3)···N(5)	3.68 (1)
N(2)···N(4)	3.94 (1)	N(4)···N(6)	3.99 (1)
C(2)···C(6)	3.87 (2)	C(6)···C(10)	3.95 (2)
C(4)···C(8)	4.46 (2)	C(8)···C(12)	4.61 (2)

Table IV. Selected Interatomic Angles in $[Rh_3(CNCH_3)_6(\mu\text{-dpmp})_2][PF_6]_3$

	At Rh(1)		
P(1)–Rh(1)–P(4)	172.4 (1)	C(1)–Rh(1)–C(3)	154.3 (6)
P(1)–Rh(1)–C(1)	85.6 (4)	P(1)–Rh(1)–C(3)	93.9 (4)
P(4)–Rh(1)–C(1)	86.9 (4)	P(4)–Rh(1)–C(3)	92.7 (4)
Rh(2)···Rh(1)–P(1)	90.7 (1)	Rh(2)···Rh(1)–P(4)	89.7 (1)
Rh(2)···Rh(1)–C(1)	88.2 (2)	Rh(2)···Rh(1)–C(3)	117.6 (2)
	At Rh(2)		
P(2)Rh(2)–P(5)	174.6 (1)	C(5)–Rh(2)–C(7)	170.0 (6)
P(2)–Rh(2)–C(5)	86.8 (3)	P(2)–Rh(2)–C(7)	92.1 (4)
P(5)–Rh(2)–C(5)	87.9 (3)	P(5)–Rh(2)–C(7)	92.9 (4)
Rh(1)···Rh(2)–P(2)	89.1 (1)	Rh(1)···Rh(2)–P(5)	90.2 (1)
Rh(1)···Rh(2)–C(5)	94.6 (2)	Rh(1)···Rh(2)–C(7)	75.4 (2)
Rh(3)···Rh(2)–P(2)	89.3 (1)	Rh(3)···Rh(2)–P(5)	89.6 (1)
Rh(3)···Rh(2)–C(5)	65.6 (2)	Rh(3)···Rh(2)–C(7)	124.4 (2)
Rh(1)···Rh(2)···Rh(3)	160.2 (1)		
	At Rh(3)		
P(3)–Rh(3)–P(6)	177.8 (1)	C(9)–Rh(3)–C(11)	166.1 (7)
P(3)–Rh(3)–C(9)	88.7 (4)	P(3)–Rh(3)–C(11)	90.6 (4)
P(6)–Rh(3)–C(9)	89.1 (4)	P(6)–Rh(3)–C(11)	91.5 (4)
Rh(2)···Rh(3)–P(3)	191.0 (1)	Rh(2)···Rh(3)–P(6)	90.4 (1)
Rh(2)···Rh(3)–C(9)	122.5 (2)	Rh(2)···Rh(3)–C(11)	71.3 (2)
	Isocyanide Ligands		
C(1)–N(1)–C(2)	173 (2)	C(7)–N(4)–C(8)	177 (2)
C(3)–N(2)–C(44)	175 (2)	C(9)–N(5)–C(6)	178 (2)
C(5)–N(3)–C(6)	173 (11)	C(11)–N(6)–C(12)	176 (2)
Rh(1)–C(1)–N(1)	168 (1)	Rh(1)–C(3)–N(2)	171 (1)
Rh(2)–C(5)–N(3)	173 (1)	Rh(2)–C(7)–N(4)	178 (1)
Rh(3)–C(9)–N(5)	176 (1)	Rh(3)–C(11)–N(6)	174 (1)
	Methylene Carbons		
P(1)–C(25)–P(2)	113.8 (6)	P(4)–C(57)–P(5)	115.2 (6)
P(2)–C(32)–P(3)	116.1 (6)	P(5)–C(64)–P(6)	115.0 (6)

absorption at 662 nm. The structure and composition of **4a** is closely related to that of the crystallographically characterized $[Rh_3(CNCH_2Ph)_{12}I_2]^{3+}$, which shows similar spectroscopic features including an intense electronic absorption in the visible (at 525 nm), but which possesses a staggered configuration of the plane of ligands at each rhodium.[19] In contrast, the bridging phosphine in **4a** limits the geometry to a nearly eclipsed orientation.

(19) Balch, A. L.; Olmstead, M. M. *J. Am. Chem. Soc.* **1979**, *101*, 3128.

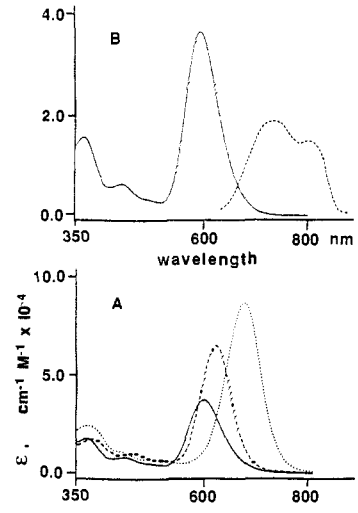

Figure 4. Trace A, the electronic absorption spectra of $[Rh_3(CNCH_3)_6(\mu\text{-dpmp})_2Cl_2][PF_6]_3$ (solid line), $[Rh_3(CNCH_3)_6(\mu\text{-dpmp})_2Br_2][PF_6]_3$ (dashed line), and $[Rh_3(CNCH_3)_6(\mu\text{-dpmp})_2I_2][PF_6]$ (dotted line) in acetone solutions. Trace B, the electronic spectra of $[Rh_3(CNCH_3)_6(\mu\text{-dpmp})_2Cl_2][PF_6]_3$ in acetone solution at 25 °C; absorption (solid line), emission (dashed line).

This and the change from isocyanide to phosphine ligands may account for the difference in energy of the absorption maxima for **4a** and $[Rh_3(CNCH_2Ph)_{12}I_2]^{3+}$. Treatment of **2** with carbon tetraiodide in acetone also produces **4a** in 93% yield.

Similar additions of chlorine or bromine to **2** occur with either the dihalogen or the corresponding carbon tetrahalide. Preparatively, the reaction with carbon tetrabromide or carbon tetrachloride is easier to accomplish, but spectroscopically identical products are obtained from dibromine or dichlorine addition. The spectroscopic properties of the products are analogous to those of **4a**.

The electronic spectra of these oxidative-addition products are compared in trace A of Figure 4. There is a decrease in energy of the dominant, low-energy electronic transition in the series Cl > Br > I, but the intensity of absorption increases in the reverse order. Very similar spectra and trends are seen for the series of mixed metal complexes $[Ir_2Au(CO)_2X_4(\mu\text{-dpma})_2]^+$.[20]

Both the chloro and bromo adducts show luminescence in dichloromethane solution. None has been detected for the corresponding iodo complex. The emission spectrum of the chloro complex **4c** is shown in trace B of Figure 4 along with the corresponding absorption spectrum. Two closely spaced emission bands at 732 and 800 nm are observed. Although it is possible that one of these emission maxima arises from an impurity, this does not appear to be the case. All samples, including carefully purified ones, exhibited the same emission features. Excitation spectra reveal that both emissions arise from irradiation at 590 nm and hence two closely spaced, emitting states must be present. The small Stokes shifts involved suggest that both features arise from fluorescence. Detector limitations prohibited us from examining the low-energy range.

Electrochemical Oxidations. A cyclic voltammogram of **2** in dichloromethane is shown in trace A of Figure 5. Two waves with $E_{1/2}$ values of 0.35 and 0.75 V (vs a silver/silver chloride reference electrode) are observed. For the first process, i_p^a/i_p^c is 1.0 as expected for a reversible process. Trace B of this figure superimposes the cyclic voltammogram of the first oxidation of **2** with that of $[Rh_2(CNC_4H_9)_4(\mu\text{-dpm})_2]^{2+}$ under identical conditions. The similarity in peak currents under identical conditions allows us to assign the oxidation process in **2** as a one-electron oxidation since previous work has identified the oxidation of $[Rh_2(CNC_4H_9)_4(\mu\text{-dpm})_2]^{2+}$ as a one-electron process.[21]

(20) Balch, A. L.; Nagle, J. K.; Oram, D. E.; Reedy, P. E., Jr. *J. Am. Chem. Soc.* **1988**, *110*, 454.

(21) Womack, D. R.; Enlow, P. D.; Woods, C. *Inorg. Chem.* **1983**, *22*, 2653.

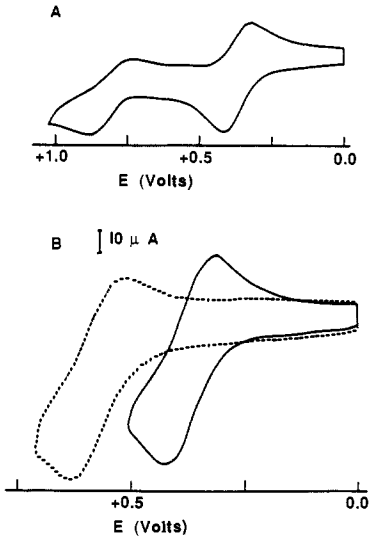

Figure 5. Trace A, cyclic voltammogram of a 0.5 mM dichloromethane solution of $[Rh_3(CNCH_3)_6(\mu\text{-dpmp})_2][PF_6]_3$ with 0.10 M tetrabutylammonium perchlorate supporting electrolyte at a scan rate of 100 mV s^{-1}. Trace B, comparison of the first oxidation waves of 0.5 mM solutions of $[Rh_3(CNCH_3)_6(\mu\text{-dpmp})_2][PF_6]_3$ (solid line) and $[Rh_2(CNBu)_4(\mu\text{-dpm})_2][PF_6]_2$ at a scan rate of 200 mV s^{-1}.

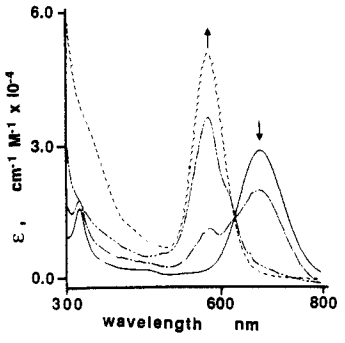

Figure 6. Electronic absorption spectra recorded during the electrolysis of a dichloromethane solution of $[Rh_3(CNCH_3)_6(\mu\text{-dpmp})_2][PF_6]_3$ at 0.4 V; initial spectrum before electrolysis (solid line), final spectrum (dashed line).

Bulk electrolysis of **2** in dichloromethane at 0.4 V leads to the formation of a violet solution whose spectroscopic properties are consistent with the formation of $[Rh_3(CNCH_3)_6(\mu\text{-dpmp})_2]^{4+}$ (**5**).[22] The electrolysis was followed by UV/visible spectroscopy. The results, shown in Figure 6, show a decrease in the 674-nm band due to **2** and the growth of a new band at 574 nm due to the new tetracation. Consistent with a one-electron oxidation, electron spin resonance spectra of the product obtained on a frozen solution at −130 °C show a broad resonance centered at $g = 2.19$. No hyperfine splitting or **g**-tensor anisotropy corresponding to that seen from the dinuclear **3** was observed.

The second oxidation process can be monitored similarly. We presume that this is the second one-electron process, although i_p^a is only 75% that of i_p^a for the first process. Electrolysis at 1.0 V in dichloromethane yields a slightly differently colored purple solution due to $[Rh_3(CNCH_3)_6(\mu\text{-dpmp})_2]^{5+}$ (**6**). The electronic spectrum of the solution after electrolysis is shown in Figure 7. The spectrum is dominated by an intense absorption at 558 nm ($\epsilon = 53\,000$ m^{-1} cm^{-1}) which is clearly distinct from the 574-nm band of the tetracation. The infrared spectrum shows a single isocyanide stretching frequency at 2215 cm^{-1}. The increase in ν(CN) is entirely consistent with oxidation.[10] No electron spin resonance spectrum was observed for the electrolyzed sample, which we presume to be diamagnetic. The chemical behavior of

(22) Weak binding of an axial ligand (i.e. perchlorate) may be involved for these species as well as for the two-electron oxidation product. Our solution data do not give specific information on this point.

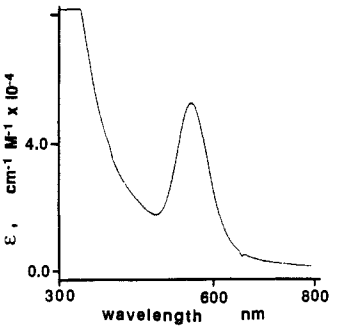

Figure 7. Final electronic absorption spectrum (assigned to $[Rh_3(CNCH_3)_6(\mu\text{-dpmp})_2]^{5+}$) obtained after electrolysis of $[Rh_3(CNCH_3)_6(\mu\text{-dpmp})_2][PF_6]_3$ in dichloromethane at 1.0 V.

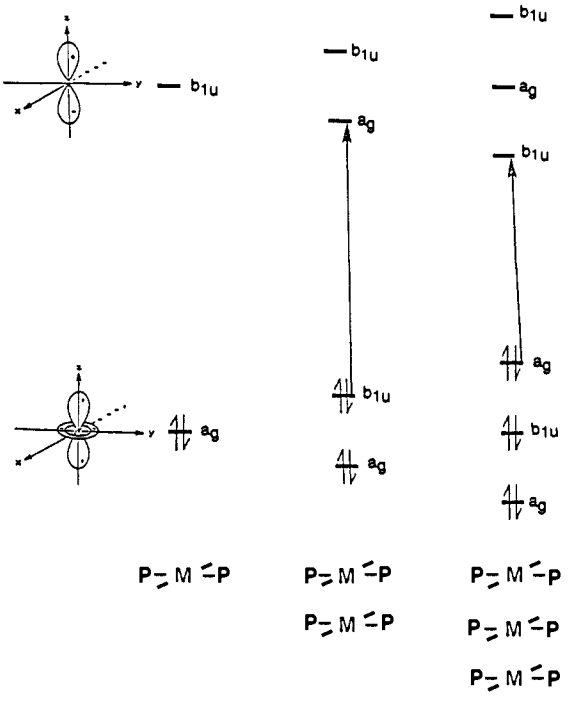

Figure 8. Molecular orbital interactions for stacking of d^8 RhP_2L_2 units in D_{2h} symmetry.

this solution is also consistent with oxidation to form $[Rh_3(CNCH_3)_6(\mu\text{-dpmp})_2]^{5+}$. Treatment of the dichloromethane solution after oxidation at 1.0 V with tetraphenylphosphonium chloride yields a blue solution with an electronic spectrum identical with that of $[Rh_3(CNCH_3)_6(\mu\text{-dpmp})_2Cl_2]^{3+}$ (**4c**). Likewise reaction with tetraethylammonium bromide or tetraethylammonium iodide produces spectral changes indicating the formation of the bromo or iodo complexes **4b** or **4a**, respectively, according to eq 2. Finally treatment of a solution of $[Rh_3(CNCH_3)_6(\mu\text{-dpmp})_2]^{5+}$

$$\underset{\mathbf{6}}{[Rh_3(CNCH_3)_6(\mu\text{-dpmp})_2]^{5+}} + 2X^- \rightarrow \underset{\mathbf{4}}{[Rh_3(CNCH_3)_6(\mu\text{-dpmp})_2X_2]^{3+}} \quad (2)$$

with **2** produces the optical spectrum characteristic of $[Rh_3(CNCH_3)_6(\mu\text{-dpmp})_2]^{4+}$ via eq 3.

$$\underset{\mathbf{6}}{[Rh_3(CNCH_3)_6(\mu\text{-dpmp})_2]^{5+}} + \underset{\mathbf{2}}{[Rh_3(CNCH_3)_6(\mu\text{-dpmp})_2]^{3+}} \rightarrow 2\underset{\mathbf{5}}{[Rh_3(CNCH_3)_6(\mu\text{-dpmp})_2]^{4+}} \quad (3)$$

Discussion

The Nature of the Rh–Rh Interactions in 2. A very simple bonding model which focuses on the overlap of the out-of-plane orbitals (the filled d_{z^2} and the empty p_z) of each rhodium(I) in **2** accounts for many of the unique spectroscopic and chemical properties of this cation. A diagram that shows the interactions

between the d_{z^2} and p_z orbitals for a series of stacked planar P_2RhL_2 units in D_{2h} symmetry is given in Figure 8. Additionally, mixing of levels of like symmetry (which is not shown in the diagram) will stabilize the filled b_{1u} and a_g (nonbonding and antibonding, respectively) so that the net Rh–Rh interaction (which has a formal bond order of zero) is attractive. Two features of this diagram are of special importance. These are the narrowing of the HOMO/LUMO gap and the rise in energy of the HOMO as the number of P_2RhL_2 units increases. Narrowing of the HOMO/LUMO gap accounts for the change in electronic spectra in the series $(Ph_3P)_2Ph(CNCH_3)_2^+$, yellow, λ_{max} = 400 nm;[10] **1**, blue violet, λ_{max} = 573 nm;[10] **2**, green, λ_{max} = 674 nm. In this case, the intense low-energy electronic transitions are assigned as an $a_g \rightarrow b_{1u}$ transition in **2** and a $b_{1u} \rightarrow a_g$ transition in **1**. The absorption spectra of the series $(Ph_3P)_2Rh(CO)Cl$, $Rh_2(CO)_2Cl_2(\mu\text{-dpm})_2$, $Rh_2(\mu\text{-Cl})(CO)_2(\mu\text{-dpm})_2^+$, and $Rh_3(\mu\text{-Cl})Cl(CO)_3(\mu\text{-dpmp})_2^+$,[11,23] and the series $Rh(CNR)_4^+$, $Rh_2(CNR)_8^{2+}$, $Rh_3(CNR)_{12}^{3+}$,[3,4] have been analyzed similarly. The emission seen for **2** is then assigned as fluorescence resulting from the $b_{1u} \rightarrow a_g$ transition. Significantly, although the trinuclear **2** and $[Rh_3(\mu\text{-Cl})Cl(CO)_3(\mu\text{-dpmp})_2]^+$ possess similar features in their electronic spectra, only **2** is luminescent.

The increase in energy of the HOMO accounts for the increase in ease of electrochemical oxidation of **2** in comparison to **1** as seen in Figure 5B. Likewise this ease of oxidation is shown in the difference in chemical behavior of **2** and **1**. Both undergo two-[10] or three-center oxidative-addition with halogens. However, **2** undergoes a thermal reaction with carbon tetrahalides to form the same product. With close analogues of **1**[24] and **1** itself, however, photochemical activation (to form an even stronger excited-state oxidant) is necessary to obtain reaction with the carbon tetrahalides.

This bonding model, which focuses on interaction of filled d_{z^2} orbitals and empty p_z orbtals, can also be extended to treat a variety of other related trinuclear complexes. Thus the mixed metal complex $[(Ir(CO)Cl)_2Au(\mu\text{-dpma})_2]^+$ (dpma is bis(diphenylphosphinomethyl)phenylarsine) contains a $d^8d^{10}d^8$ IrAuIr chain which shows structural and spectroscopic features (including luminescence) that are similar to **2**.[20] Both $[(Ir(CO)Cl)_2Tl(\mu\text{-dpma})_2]^+$ and $[(Ir(CO)Cl)_2Pb(\mu\text{-dpma})_2]^{2+}$ contain IrTlIr or IrPbIr chains in which a filled s^2 orbital plays a similar role as the filled d_{z^2} orbital on the central rhodium of **2**.[26] $Tl_2Pt(CN)_4$ contains a $s^2d^{10}s^2$, Tl–Pt–Tl chain whose bonding has been described in related fashion.[27]

Finally we note that within the group of compounds described here, we have detected only terminal isocyanide ligands both in solution and in the solid state. There is no evidence that any of these particular complexes fold about a single isocyanide to form the novel triply bridging isocyanide found in the solid state form of $[Rh_3(n\text{-BuNC})_5(CO)(\mu\text{-dpmp})_2]^{3+}$ (**7**).[27]

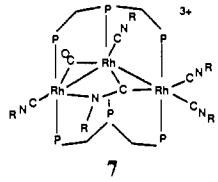

7

Experimental Section

Preparation of Compounds. Methyl isocyanide[28] and $[Rh_3(CO)_3(\mu\text{-Cl})Cl(\mu\text{-dpma})_2][BPh_4]$[14] were prepared by published procedures. All reactions were carried out in dioxygen-free solvents under a dinitrogen atmosphere.

Table V. Crystal Data and Data Collection Parameters for $[Rh_3(MeNC)_6(\mu\text{-dpmp})_2][PF_6]_3\cdot 1.3CH_2Cl_2$

formula	$C_{79}H_{82}N_6F_{18}P_9Cl_6Rh_3$ (assumes three molecules of CH_2Cl_2)
fw	2257.67
color and habit	green plates
cryst syst	triclinic
space group	$P\bar{1}$
a, Å	14.111 (4)
b, Å	16.65 (5)
c, Å	21.644 (6)
α, deg	91.42 (2)
β, deg	102.43 (2)
γ, deg	103.71 (2)
V, Å^{-3}	4810 (3)
T, deg	130
Z	2
cryst dimens, mm	0.57 × 0.62 × 0.11
d_{calcd}, g cm^{-3}	1.56
radiation (Å)	Mo Kα (λ = 0.71069)
μ(Mo Kα), cm^{-1}	7.5
range of transmission factors	0.69–0.93
diffractometer	$P2_1$, graphite monochromator
scan method	ω, 1.2° range, 1.2° offset for bkgnd
scan speed, deg min^{-1}	15
2θ range, deg	0–45
octants collected	$h,\pm k,\pm l$
no. of data collected	12469
no. of unique data	12469
no. of data used in refinement	8971 [$I > 3\sigma(I)$]
no. params refined	826
R^a	0.095
$R_w{}^a$	0.107 [$w = 1/\sigma^2(F_o)$]

$^a R = \sum||F_o| - |F_c||/|F_o|$ and $R_w = \sum||F_o| - |F_c||w^{1/2}/\sum|F_o w^{1/2}|$.

$[Rh_3(CNCH_3)_6(\mu\text{-dpmp})_2][PF_6]_3$. Methyl isocyanide (33 μL, 0.56 mmol) was added dropwise with stirring to a rose-colored solution of 150 mg (0.084 mmol) of $[Rh_3(CO)_3(\mu\text{-Cl})Cl(\mu\text{-dpmp})_2][BPh_4]$ in 5 mL of dichloromethane. Addition of 500 mg (3.0 mmol) of ammonium hexafluorophosphate in 15 mL of methanol to the resulting green solution produced green crystals. The volume of the solution was reduced by vacuum evaporation to ensure complete precipitation. The product was collected by filtration and washed with methanol and ethyl ether. It was dissolved in a minimum of dichloromethane, and the solution was filtered to remove a small amount of an unidentified purple solid. The product was reprecipitated by adding a solution of 150 mg of ammonium hexafluorophosphate in 20 mL of methanol. Precipitation was completed by removal of some of the solvent by vacuum evaporation. The green, crystalline solid was collected by filtration and washed with methanol and ethyl ether; yield, 104 mg (62%). Anal. Calcd for $C_{76}H_{76}F_{18}N_6P_9Rh_3$: C, 45.57; H, 3.82; N, 4.20. Found: C, 45.11; H, 3.72; N, 4.21.

$[Rh_3(CNCH_3)_6(\mu\text{-dpmp})_2I_2][PF_6]_3$. Method 1. A solution of 12.5 mg (0.049 mmol) of iodine in 1 mL of acetone was added dropwise to a solution of 50 mg (0.025 mmol) of $[Rh_3(CNCH_3)_6(\mu\text{-dpmp})_2][PF_6]_3$ in 2 mL of acetone. Slow addition of ethyl ether to the green solution gave green crystals of the product. This was collected by filtration, washed with ethyl ether, and recrystallized from acetone/ethyl ether; yield, 53 mg (94%).

Method 2. A solution of 10 mg (0.019 mmol) of carbon tetraiodide in 1 mL of acetone was added dropwise to a solution of 20 mg (0.010 mmol) of $[Rh_3(CNCH_3)_6(\mu\text{-dpmp})_2][PF_6]_3$ in 1 mL of acetone. After the addition of diethyl ether, the green crystalline product was treated as described in Method 1, to give 21 mg (93%) of product. Anal. Calcd for $C_{76}H_{76}F_{18}I_2N_6P_9Rh_3$: C, 40.45; H, 3.39; N, 3.72; I, 11.25. Found: C, 39.53; H, 3.33; N, 3.65; I, 10.98.

$[Rh_3(CNCH_3)_6(\mu\text{-dpmp})_2Br_2][PF_6]_3$. This blue-green crystalline solid was prepared in 96% yield from carbon tetrabromide by using Method 2, above. Anal. Calcd for $C_{76}H_{76}Br_2F_{18}N_6P_9Rh_3$: C, 42.20; H, 3.54; N, 3.89. Found: C, 41.87; H, 3.49; N, 3.74.

$[Rh_3(CNCH_3)_6(\mu\text{-dpmp})_2Cl_2][PF_6]_3$. Blue crystals were obtained in 82% yield from carbon tetrachloride by using Method 2, described above, for the corresponding iodide. Anal. Calcd for $C_{76}H_{76}Cl_2F_{18}N_6P_9Rh_3$: C, 44.01; H, 3.69; N, 4.05. Found: C, 43.95; H, 3.65; N, 3.86.

Physical Measurements. The ^{31}P NMR spectra were recorded with proton decoupling on a Nicolet NT-200 Fourier transform spectrometer operating at 81 MHz, or on a Nicolet NT-360 at 146 MHz. The reference was external 85% phosphoric acid. The high-frequency-positive

(23) Balch, A. L.; Fossett, L. A.; Olmstead, M. M.; Reedy, P. E., Jr. *Organometallics* **1986**, *5*, 1929.
(24) Che, C.-M.; Lee, W.-M. *J. Chem. Soc., Chem. Commun.* **1986**, 616.
(25) Balch, A. L.; Nagle, J. K.; Olmstead, M. M.; Reedy, P. E., Jr. *J. Am. Chem. Soc.* **1987**, *109*, 4123.
(26) Nagle, J. K.; Balch, A. L.; Olmstead, M. M. *J. Am. Chem. Soc.* **1988**, *110*, 319.
(27) Balch, A. L.; Fossett, L. A.; Olmstead, M. M. *Organometallics* **1987**, *6*, 1827.
(28) Schuster, R. E.; Scott, J. E.; Casanova, J., Jr. *Org. Synth.* **1966**, *46*, 75.

convention, recommended by IUPAC, has been used in reporting all chemical shifts. Infrared spectra were recorded from mineral oil mulls or dichloromethane solutions with a Perkin-Elmer 180 or IBM IR32 spectrometer. Electronic spectra were recorded on a Hewlett-Packard 8450A spectrophotometer. Emission spectra were recorded on a Perkin-Elmer MPF-44B fluorescence spectrophotometer. Electrochemical measurements were made with an EG&G Princeton Applied Research Model 173 potentiosat/galvanostat with a Model 179 digital coulometer plug-in. For cyclic voltammetric measurements a Model 175 universal prorammer was used also. All potentials reported are for degassed dichloromethane solutions containing 0.5 mM compound and 0.1 *M* tetrabutylammonium perchlorate. An Ag/AgCl reference electrode was used in all measurements. The ferrocenium/ferrocene potential was measured as 0.49 (1) V under these conditions.

X-ray Structure Determination and Refinement. Well-formed green plates were obtained from a green dichloromethane solution of the complex which was layered with 1 drop of methanol followed by several mL of diethyl ether. The crystals were handled while immersed in a hydrocarbon oil in order to retard loss of lattice solvent and prevent fracture. A suitable crystal was mounted on a glass fiber with use of silicone grease and placed in the cold stream of the diffractometer. No decay in the intensities of two standad reflections was observed during the course of data collection. Crystal data and information regarding data collection are given in Table V.

The usual corrections for Lorentz and polarization effects were applied to the data. Crystallographic programs used were those of SHELXTL, version 4, installed on a Data General Eclipse computer. Scattering factors and corrections for anomalous dispersion were from the *International Tables*.[29]

Solution of the structure was accomplished by a combination of Patterson and Fourier methods. The species of interest, the trirhodium cation, displays no disorder. However, the structure exhibits disorder in the remaining region of the crystal lattice. Although only three PF_6^- groups are required by stoichiometry, there are actually four sites (some with partial occupancy) for these anions. All of these PF_6^- groups have different types of disorder. This is depicted in a figure in the supplementary material. In addition there are three partially occupied sites for molecules of dichloromethane. Figure 2 of the supplementary material is a stereoview of the region of the lattice that contains these disordered molecules.

Six low-angle reflections affected by extinction were omitted from the data. An absorption correction was applied.[30] In the final cycles of refinement, rhodium, phosphorus, fluorine, and chlorine (except Cl(6a and b)) atoms were assigned anisotropic thermal elipsoids. Hydrogen atoms in the cation were included in the structure factor calculation by use of a riding model, with C-H of 0.96 Å and $U_{iso} = 1.2U_{iso}$ for the bonded carbon. In the final difference map there were several features of ca. 1.0 eÅ^{-3} in height, all in the region of the disordered anions and dichloromethane. In view of the severe disorder present, the final *R* value of 0.095 is not unreasonable.

Acknowledgment. We thank the National Science Foundation (Grant CHE 8519557) for financial support, Bowdoin College for faculty study leave for J.K.N., and Johnson Matthey for a loan of rhodium salts.

Registry No. 2, 115559-93-8; **2**·1.3CH_2Cl_2, 115649-39-3; **4a**, 115590-24-4; **4b**, 115559-95-0; **4c**, 115559-97-2; **5**, 115559-98-3; **6**, 115590-25-5; $[Rh_3(CO)_3(\mu\text{-Cl})Cl(\mu\text{-dpmp})_2][BPh_4]$, 84774-75-4.

Supplementary Material Available: Listings of all bond distances, bond angles, hydrogen atom positions, and anisotropic thermal parameters and figures showing the disordered regions (11 pages); listing of structure factors (53 pages). Ordering information is given on any current masthead page.

(29) *International Tables for X-ray Crystallography*; Kynoch Press: Birmingham, England, 1974; Vol. IV.

(30) The program XABS obtains an absorption tensor from $F_o - F_c$. Hope, H.; Moezzi, B., Department of Chemistry, University of California, Davis, CA.

Rational Design in Homogeneous Catalysis. Ir(I)-Catalyzed Addition of Aniline to Norbornylene via N-H Activation

Albert L. Casalnuovo,* Joseph C. Calabrese, and David Milstein‡

Contribution No. 4635 from E. I. du Pont de Nemours & Co., Inc., Central Research & Development Department, Experimental Station, Wilmington, Delaware 19898.
Received February 8, 1988

Abstract: The first successful demonstration of the amination of an olefin by a transition-metal-catalyzed N-H activation mechanism was accomplished in a stepwise manner with an Ir(I) catalyst and the substrates aniline and norbornylene. The initial N-H oxidative addition step envisioned in such a mechanism was demonstrated for the complexes $Ir(PMe_3)_4PF_6$, $Ir(PMe_3)_3(C_8H_{14})Cl$, and $Ir(PEt_3)_3Cl$, all of which gave rise to stable cis anilido hydride complexes when reacted with aniline. The second step, olefin insertion, was accomplished from the reaction of $Ir(PEt_3)_2(C_2H_4)_2Cl$ (**1**) with aniline and norbornylene. The resulting insertion product, $Ir(PEt_3)_2(NHPhC_7H_{10})(H)Cl$ (**6**), was characterized by NMR spectroscopy and single-crystal X-ray diffraction and was found to have an azoiridacyclobutane type structure. The relevant crystal data for **6** are $a = 10.702$ (3) Å, $b = 13.176$ (21) Å, $c = 19.498$ (5) Å, $\beta = 98.61$ (2); $P2_1/c$, $T = -70$ °C, $d_c = 1.591$ g/cm^3, $\mu = 51.21$ cm^{-1}; 3029 reflections, $R = 0.039$ and $R_w = 0.036$. Decomposition studies of **6** established two competing reaction pathways. C-N and Ir-C bond breaking, the microscopic reverse of the formation of **6**, gave norbornylene and a reactive Ir intermediate. The competing pathway of C-H reductive elimination occurs by prior ligand dissociation and yields the amination product, *exo*-2-(phenylamino)norbornane (**7**). Labeling studies indicated an overall cis addition of the N-H group across the exo face of norbornylene. The individual steps for this reaction were elaborated into a catalytic cycle for the addition of aniline to norbornylene and a mechanism based on these individual steps proposed.

Rational design of transition-metal homogeneous catalysis is an attractive but generally difficult goal to accomplish. Our initial results on the activation of ammonia by an electron-rich Ir complex prompted us to investigate such a design for the amination of olefins.[1] Here we report on the results of this study, leading to the first successful demonstration of the catalytic amination of an olefin by N-H activation.

Transition-metal-promoted amination of olefins is generally stoichiometric and is based on nucleophilic attack of a free amine on an olefin coordinated to a high-valent metal center.[2] A

‡Department of Organic Chemistry, Weizmann Institute of Science, Rehovot, Israel 76100.

(1) Casalnuovo, A. L.; Calabrese, J. C.; Milstein, D. *Inorg. Chem.* **1987**, *26*, 971.

0002-7863/88/1510-6738$01.50/0